



*LIGO Laboratory / LIGO Scientific Collaboration*

LIGO-T1000517-v5

*LIGO*

11/17/10

---

**Optical levers Final Design Review for test masses,  
recycler mirrors and HAM optical benches**

---

Riccardo Desalvo, Eric Black, Norris Kilpatrick, Gerardo Moreno, Ignacio Romero, and Mohana Mageswaran

Distribution of this document:  
LIGO Scientific Collaboration

This is an internal working note  
of the LIGO Laboratory.

**California Institute of Technology**  
**LIGO Project – MS 18-34**  
**1200 E. California Blvd.**  
**Pasadena, CA 91125**  
Phone (626) 395-2129  
Fax (626) 304-9834  
E-mail: [info@ligo.caltech.edu](mailto:info@ligo.caltech.edu)

**Massachusetts Institute of Technology**  
**LIGO Project – NW22-295**  
**185 Albany St**  
**Cambridge, MA 02139**  
Phone (617) 253-4824  
Fax (617) 253-7014  
E-mail: [info@ligo.mit.edu](mailto:info@ligo.mit.edu)

**LIGO Hanford Observatory**  
**P.O. Box 159**  
**Richland WA 99352**  
Phone 509-372-8106  
Fax 509-372-8137

**LIGO Livingston Observatory**  
**P.O. Box 940**  
**Livingston, LA 70754**  
Phone 225-686-3100  
Fax 225-686-7189

<http://www.ligo.caltech.edu/>

## 1 Scope and Introduction

Optical levers will be used to monitor the alignment of all the large, suspended optics and most of the HAM tables. Each lever consists of a light source, receiver, and associated mounting hardware and focusing telescopes. The design of the subsystem encompasses each of these areas and will be described in this document. In particular, the design covers the following.

Optical components:

- The light sources, 4 mW, visible diode lasers,
- Transport fibers to carry the light from the lasers to the focusing telescopes, and
- The focusing, or launching telescopes themselves.

Electrical:

- The receiver quadrant photodetectors (QPDs),
- The transimpedance amplifier, that converts the QPDs photocurrent to a measureable voltage, and
- Electrical connections and signal cables that route the output of the receivers to the delivery point of the data acquisition system, and
- Controllers and associated cabling for the motors used to center the light spots on the QPDs.

Mechanical:

- Mounting pylons for both transmitters (light sources) and receivers,
- Tip/tilt telescope aiming mechanisms, and
- Stepper or pico-motor micrometric positioners for the quadrant photodiodes.

The optical levers can be grouped into four types.

- Test-mass optical levers,
- Recycling mirror optical levers,
- HAM-table optical levers, and
- Beamsplitter and folding-mirror optical levers.

The first two are topologically similar, with separate launching and receiving pylons and their respective telescopes and receiving QPDs. The last two have the transmitters and receivers mounted on the same platform. The HAM-table levers have both their transmitters and receivers mounted on the same pylon, but the beamsplitter and folding-mirror levers are mounted on separate platforms attached to the vacuum system and do not use free-standing pylons. As their name implies, the HAM-table optical levers monitor the orientations of the optical tables inside the HAM chambers, rather than those of suspended mirrors.

This final design review is limited to the optical levers of test masses, recycler mirrors, and HAM tables, i.e. those levers that mount on pylons. Excluded are the optical levers for the beam splitters and folding mirrors, which will be treated in a separate document. The rationale for this grouping is

to include all optical levers with external pylons so that the pylons can all be procured at the same time.

## 1.1 Changes since the PDR

Although the preliminary design review proposed so far [T1000219](#) was formally restricted to the test mass optical levers, there are no significant differences or changes with respect to the preliminary design review, except for the quadrant photodiode centering mechanism, which remains based on stepper motor linear movements for the large mirror receiver diodes. The HAM, the beamsplitter, and the folding mirror optical levers will re-use the pico-motor-driven tip/tilt mechanism already in use in present LIGO. The model [D1001515](#) illustrates the design of this mechanism for the HAM levers.

The question of laser vs. SLED as a light source has been resolved in favor of the lasers. Dennis Coyne did a trade study to inform his decision, and his writeup is posted in the dcc at [T1000390](#).

## 2 Requirements and Specifications

This is a summary of what is given in prior documents and is essentially unchanged from the PDR and the DRD. The following list is taken from [G1000451](#) and is about as succinct as it gets.

The purpose of the optical levers subsystem are,

1. To assist in restoring alignment after invasive work,
2. To tune the test mass actuators to minimize position-to-angle coupling
3. Monitor the angular alignment of the HAM optical tables
4. Local pitch and yaw mode damping during interferometer commissioning (not in science mode)
5. Risk reduction research – monitor thermal distortion of tests mass radius of curvature with three beams

The optical lever signal should be stable to within 1 micro-radian over a time span of one hour, and they should display a position-to-angle coupling of no more than 100 nano-radians per micron.

Note that the aLIGO optical levers are *not* intended to be used for local damping with the interferometer in science mode, as the iLIGO levers are currently employed. This is a consequence of the more stringent noise requirement for aLIGO. In the design process for the advanced-LIGO levers, we estimated how good a servo we would need to damp the optics' angular motion without spoiling the overall noise budget of the instrument. Specifically, we calculated how much attenuation we would need in the interferometer signal band to keep an optical-lever servo from injecting ground noise into its associated suspended optic, and how fast the servo gain should roll off above the highest mechanical resonance of the suspension system. Such a servo would not have been impossible to build, but it would have been challenging. We showed the calculations to Peter Fritschel, and he said, "If it's going to be that hard, don't do it." His rationale was that active local damping could just as well be done using WFS, and building such a capability into optical levers added unnecessary complexity to the subsystem.

### 3 Resolution of Action Items from PDR

Refer to the “Findings” section of the Advanced LIGO Review Committee Report: Test Mass Optical Lever PDR [M1000142](#).

There were five findings, not all of which were action items.

- 1) The committee recommends re-using Initial LIGO visible OpLev lasers. The lifetime of the current iLIGO oplev lasers is sufficiently good such that they can form the light source for the baseline design. The committee does not find the reasons given for IR SLEDs (lifetime, spot interference) sufficiently good to justify their inclusion into the design, in light of their subsequent safety and convenience issues, and lack of proven performance.
  - Duly noted and accepted. ALIGO optical levers will use visible lasers.
- 2) Visible SLEDs can be tested, time-permitting, in bench settings and at the 40m lab for example, for future retrofit in aLIGO if their performance and lifetime warrants this.
  - Sounds like a fine thing to do, after the aLIGO optical levers are installed and tested.
- 3) The choice of Hamamatsu QPD looks workable, provided there is close coupling with the CDS group regarding amplifier and readout electronics.
  - Duly noted and accepted. We are proceeding with the design using the Hamamatsu photodiodes.
- 4) Electronics descriptions and drawings are required for expected signals and noise levels, readout, sign conditioning, DAQ etc. These must be provided to the CDS group (working in concert with the CDS representatives to the oplev design team).
  - Duly noted and covered in this review.
- 5) Mechanical design. The review team would like to clarify with the design team regarding the robustness and flexibility of the following mechanical issues in the test mass oplev design: i) adjustability of the pylon attachment at the floor, ii) clearance/stay clear issues when setting the pylons, and iii) mechanical rigidity of the pylon once the mass of the optical table and launching hardware is mated to the thinner apex region of the triangular structure.
  - Done. Addressed below.

### 4 Design Summary

The initial-LIGO levers are almost good enough to be used as-is in advanced LIGO. If we were planning on using the levers for active damping of the suspended optics in science mode, we would need a need to improve the optical and electronic performance of the subsystem, but since we're not, the existing levers would handily meet the advanced-LIGO requirements. The only thing about the existing levers that needs to be to be changed is the collection of pylons they mount on. The existing pylons are not in the right places and don't have the right heights to “see” the advanced-

LIGO optics. The original pylons, in addition to being the wrong size for advanced LIGO, suffer from several other weaknesses as well. They are quite sensitive to acoustic and mechanical noise, for example, in addition to being heavy and unwieldy. As long as we are replacing them, we might as well improve on their design. The light sources and receivers are largely unchanged from initial-LIGO, with one notable exception that we will describe below.

## 4.1 Mechanical design

The original pylons were top-heavy and suffered from the weakness of their connection to ground. Light pyramidal pylons, getting their rigidity from folded sheet metal structure and grouted to the floor were designed. This represents more than an order of magnitude improvement over initial LIGO. Constrained-layer damping material is added to the sheet metal to suppress mechanical resonances.

The pylons can be divided into three types.

- Launching pylons: Whenever the light source and receiver are mounted on separate pylons, launching is always made from the lowest pylon and receiving from the taller one. This minimizes sensitivity to vibrations and seismic motion. All of the dedicated launching pylons are less than 60 cm tall.

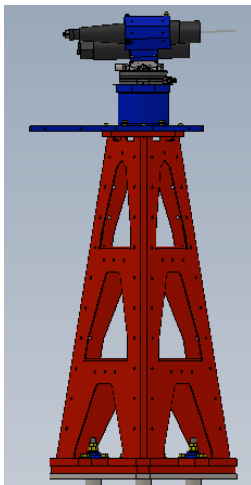


**Figure 1: Example of a dedicated launcher pylon. This one is for the test-mass optical levers.**

- Receiving pylons: The receiver pylons for the test masses and for the recycler mirrors have to reach viewports above the beam line. To do this they must be substantially taller than the launching pylons and are typically between 2.5 and 3 meters tall. They are also tilted to reach the required viewports over the beam pipe. Both exist in right- and left-handed versions.

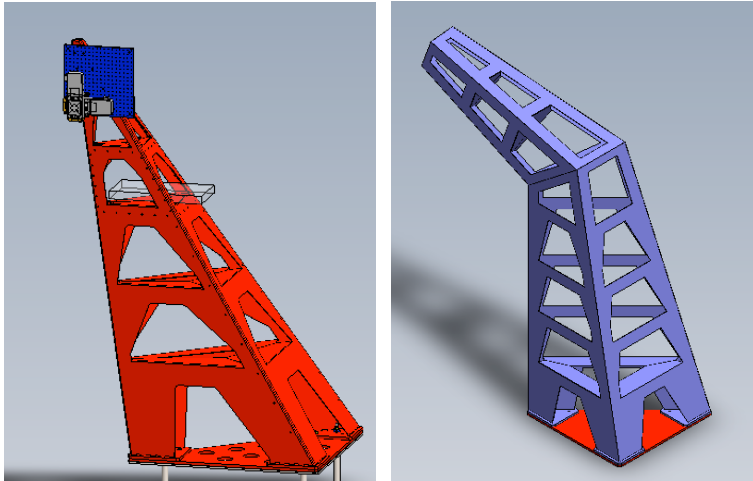


**Figure 2: Examples of test-mass (red) and recycler (blue) receiving pylons.**

- HAM-table pylons: The pylons for the HAM tables will be both transmitter and receiver. The beam reflects on a mirror mounted on a tuable tip/tilt mechanism mounted on the HAM table and adjusted manually to return to the launching viewport. Steering of the beam on the center of the QPD is achieved with a picomotor tip/tilt stage.

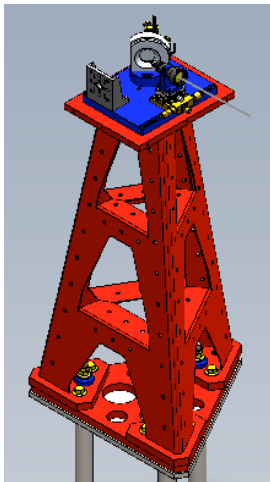


**Figure 3: Example of a HAM-table pylon. Both transmitter and receiver mount on the same platform here.**

Each pylon includes a breadboard positioned at its business end. Receiving pylon breadboards carry an XY stepper motor stage to position the center of the QPD on the arriving beam spot. Normally-locked brakes protect from accidental change of positioning. A Mitutoyo position sensor (similar to a caliper) provides permanent memory of the positioning of the QPD. Cabling for signal and motor controls and position readout will extend to a reserved optical lever rack space of location to be determined. Controls will be only local, using a transportable stepper-motor control unit.

All pylons are bolted to a steel platform grouted to the floor to maximize rigidity. The beamsplitter and folding mirror optical levers (to be covered in a separate review) will be mounted on an

existing BSC blue pier and will incorporate both transmitter and receiver similar to the HAM pylons.

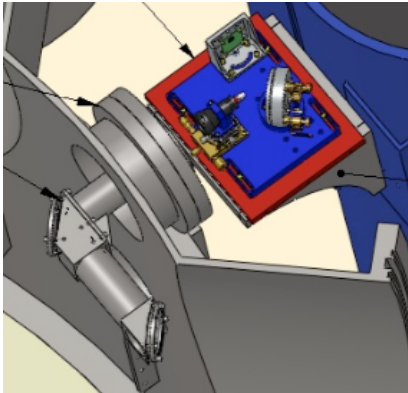


**Figure 4: Beamsplitter and folding-mirror transmitter and receiver platform. These do not mount on pylons and are included here for information only. Note the in-vacuo periscope inside the viewport.**

## 4.2 Optical design

The initial-LIGO source consisted of a commercial, fiber-coupled diode laser, followed immediately by an adjustable beam expander and collimator. The expander/collimator was also a commercial item and was reminiscent of the telephoto lenses used with single-lens-reflex cameras, where adjustments to the beam diameter at the receiver (i.e. the focus) were made by turning an adjustable ring around the barrel of the unit. Immediately after this, there was a steering mirror that launched the beam to the target suspended mirror. We identified two problems with this design.

- Placing the steering mirror after the beam expander necessitated a fairly large steering mirror. In spite of the large mirror, the edge of the beam routinely got clipped, and this clipping was a significant source of coupling between mechanical noise in the launching structure and the shape of the spot. At the receiver, this looked like noise in the position of the spot or noise in the orientation of the suspended optic. We solved this problem by eliminating the steering mirror. We retain the beam-expanding telescope, but it is now mounted directly on a rigid tip/tilt stage for steering the outgoing beam.
- Vibrations on the fiber feeding to the launcher telescope were found to generate beam jitter on the order of several microradians, well outside our specs. The problem was traced to light backscattered to the laser, causing it to jump modes. Mode jumping caused differences in the light injection in the fiber. This would not represent a problem in a truly monomode fiber. The problem is that our “monomode” fibers are true monomode fibers only over distances of kilometers. In the several meters of distance used in the LVEA, more than one mode gets transmitted. The interference of the modes exiting the fiber caused the launched beam angle to move by several microradians. Specifically, the reflections occur at the end of the fiber, where the surface is perpendicular to the fiber’s axis. Using angle-cut fibers, where the end of the fiber is cut at approximately Brewster’s angle to the fiber axis, seems to have eliminated this problem. We can now wiggle the fiber all we want and see very little measureable beam jitter in response. It is perhaps significant that we do *not* see *no* microphonic coupling with angle cut fibers. The launching angle of the fiber remains

sensitive to spontaneous laser-mode shifting. One possible solution to this would be to replace the laser light sources with superluminescent LEDs, which emit incoherent light and would likely not produce the problematic interference effect. This would motivate research into SLEDs as suggested in Finding 2 of the review committee's response to the PDR, but it has no bearing on the present design. Although spontaneous mode jumping does result in an angular shift of the beam that is well outside spec, we estimate that this is a sufficiently rare event that we can proceed with the current design.

### 4.3 Electronics design

The electronics associated with the light source, the tip/tilt steering mechanism, and the XY positioning stages for the receivers are all commercial items. The only electronics requiring in-house design and construction are those associated with converting the QPD photocurrent to a useable voltage. The preamplifier used in initial LIGO was largely adequate, and we have essentially just repackaged that to satisfy the different geometrical constraints. The only significant change is a switch to lower-noise photodiodes to replace the now-obsolete diodes currently in use.

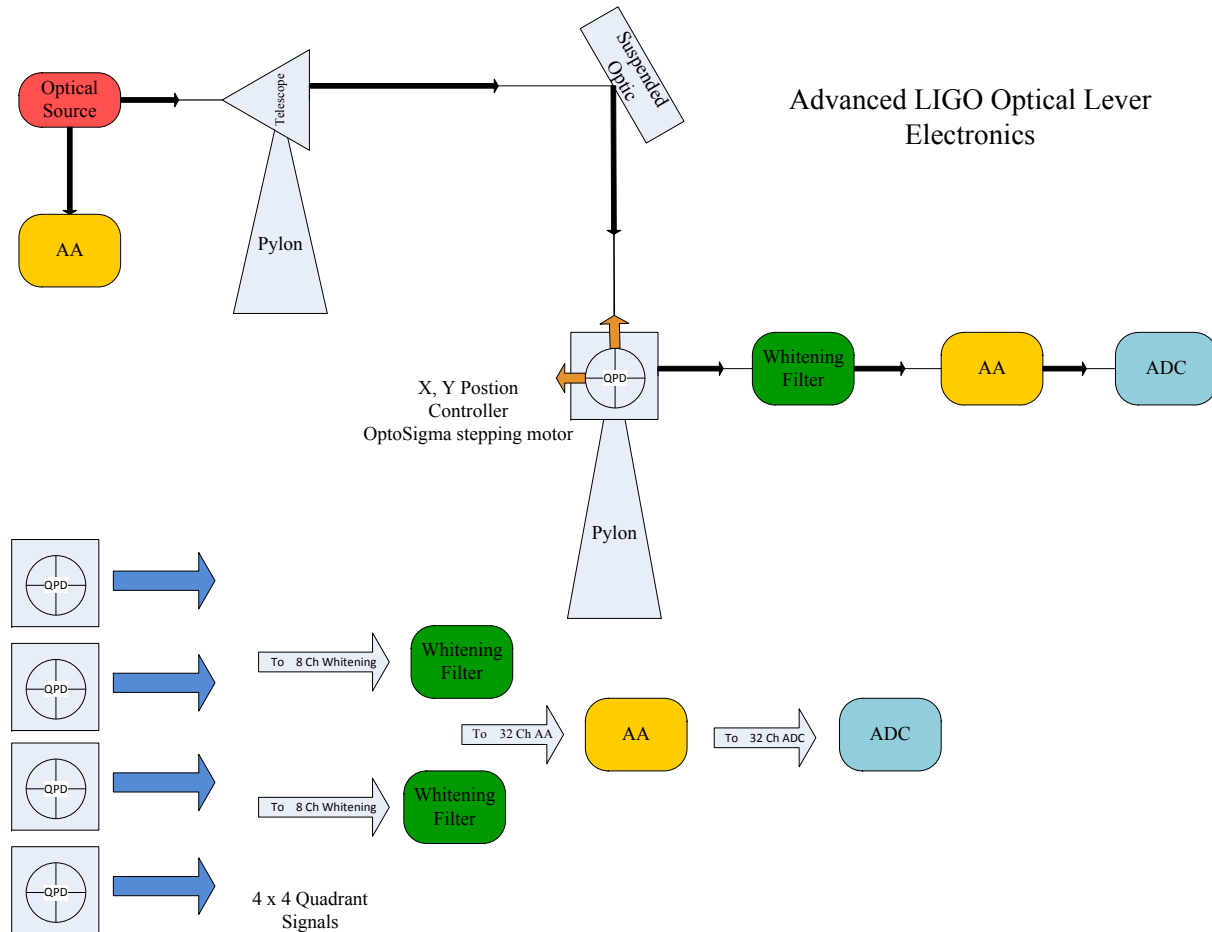


**Figure 5: Block diagram of the optical-lever electronics.**

IFO	Optic	Chamber	Flange Type	Location	In Viewport	Out Viewport	Building
H1	IMTX	BSC3	A1-A	Facing chamber	VP3	VP6	LVEA
H1	ITMY	BSC1	A1-B	Facing chamber	VP4	VP1	LVEA
H1	ETMX	BSC9	A1-A	Facing chamber	VP4	VP1	X END
H1	ETMY	BSC10	A1-B	Facing chamber	VP3	VP6	Y END
H1	BS	BSC2	N/A	On chamber	G2	G2	LVEA
H1	PR3	HAM2	MC Tube	WAMCB1	VP7	VP11	LVEA
H1	SR3	HAM5	MC Tube	WAMCB2	VP5	VP1	LVEA
H1	HAM2 Mirror	HAM2	MC Tube	WAMCB1	VP5	VP5	LVEA
H1	HAM3 Mirror	HAM3	MC Tube	WAMCA1	VP5	VP5	LVEA
H1	HAM4 Mirror	HAM4	MC Tube	WAMCA2	VP5	VP5	LVEA
H1	HAM5 Mirror	HAM5	MC Tube	WAMCB2	VP7	VP7	LVEA
H2	ITMX	BSC7	A1-A	Facing chamber	VP4	VP1	LVEA
H2	ITMY	BSC8	A1-B	Facing chamber	VP3	VP6	LVEA
H2	ETMX	BSC5	Flat-Faced	Facing chamber	VP4	VP6	X END
H2	ETMY	BSC6	Flat-Faced	Facing chamber	VP5	VP1	Y END
H2	BS	BSC4	N/A	On chamber	G8	G8	LVEA
H2	PR3	HAM8	MC Tube	WAMCB3	VP6	VP12	LVEA
H2	SR3	HAM11	MC Tube	WAMCB4	VP7	VP11	LVEA
H2	HAM8 Mirror	HAM8	MC Tube	WAMCB3	VP5	VP5	LVEA
H2	HAM9 Mirror	HAM9	MC Tube	WAMCA3	VP5	VP5	LVEA
H2	HAM10 Mir.	HAM10	MC Tube	WAMCA4	VP5	VP5	LVEA
H2	HAM11 Mir.	HAM11	MC Tube	WAMCB4	VP5	VP5	LVEA
H2	FMX	BSC7	N/A	On chamber	G5	G5	LVEA
H2	FMY	BSC8	N/A	On chamber	G8	G8	LVEA
L1	ITMX	BSC3	A1-A	Facing chamber	VP3	VP6	LVEA
L1	ITMY	BSC1	A1-B	Facing chamber	VP4	VP1	LVEA
L1	ETMX	BSC4	A1-A	Facing chamber	VP4	VP1	X END
L1	ETMY	BSC5	A1-B	Facing chamber	VP3	VP6	Y END
L1	BS	BSC2	N/A	On chamber	G2	G2	LVEA
L1	PR3	HAM2	MC Tube	LAMCB1	VP7	VP11	LVEA
L1	SR3	HAM5	MC Tube	LAMCB2	VP5	VP1	LVEA
L1	HAM2 Mirror	HAM2	MC Tube	LAMCB1	VP5	VP5	LVEA
L1	HAM3 Mirror	HAM3	MC Tube	LAMCA1	VP5	VP5	LVEA
L1	HAM4 Mirror	HAM4	MC Tube	LAMCA2	VP5	VP5	LVEA
L1	HAM5 Mirror	HAM5	MC Tube	LAMCB2	VP7	VP7	LVEA

**Figure 6: List of optical levers by target and location.**

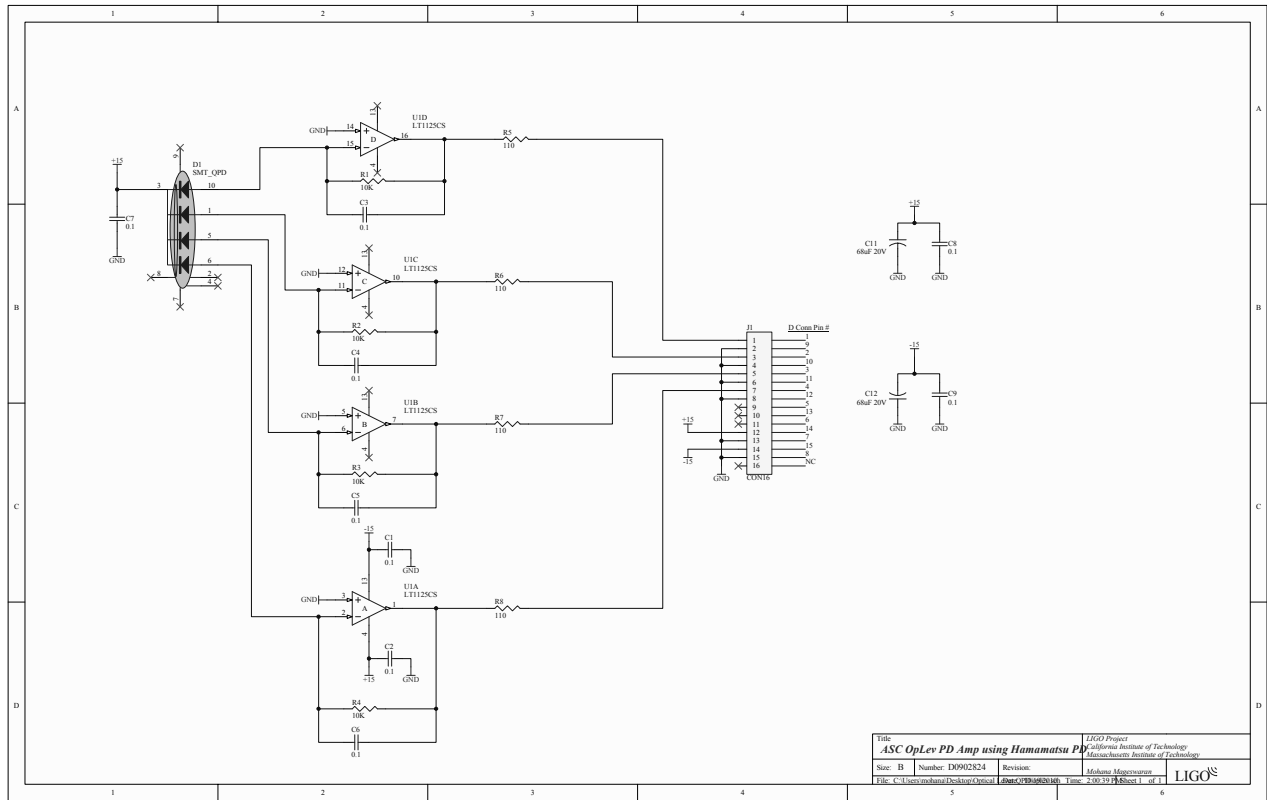


Figure 7: Schematic of QPD current-to-voltage preamplifier electronics.

## 4.4 Interfaces

### 4.4.1 Floor occupancy

A sketch of the layout inside the LVEA is shown in Figure 8. This configuration applies to all three interferometers. In H2, there are also levers on the folding mirrors.

Figures 9-14 show the actual floor layout, with comments in red. Riccardo visited both sites and did a walkthrough to make sure the drawings and models were representative of what's really there.

Note that this floor occupancy may change, depending on input from TCS, etc., but that is beyond the scope of this review.

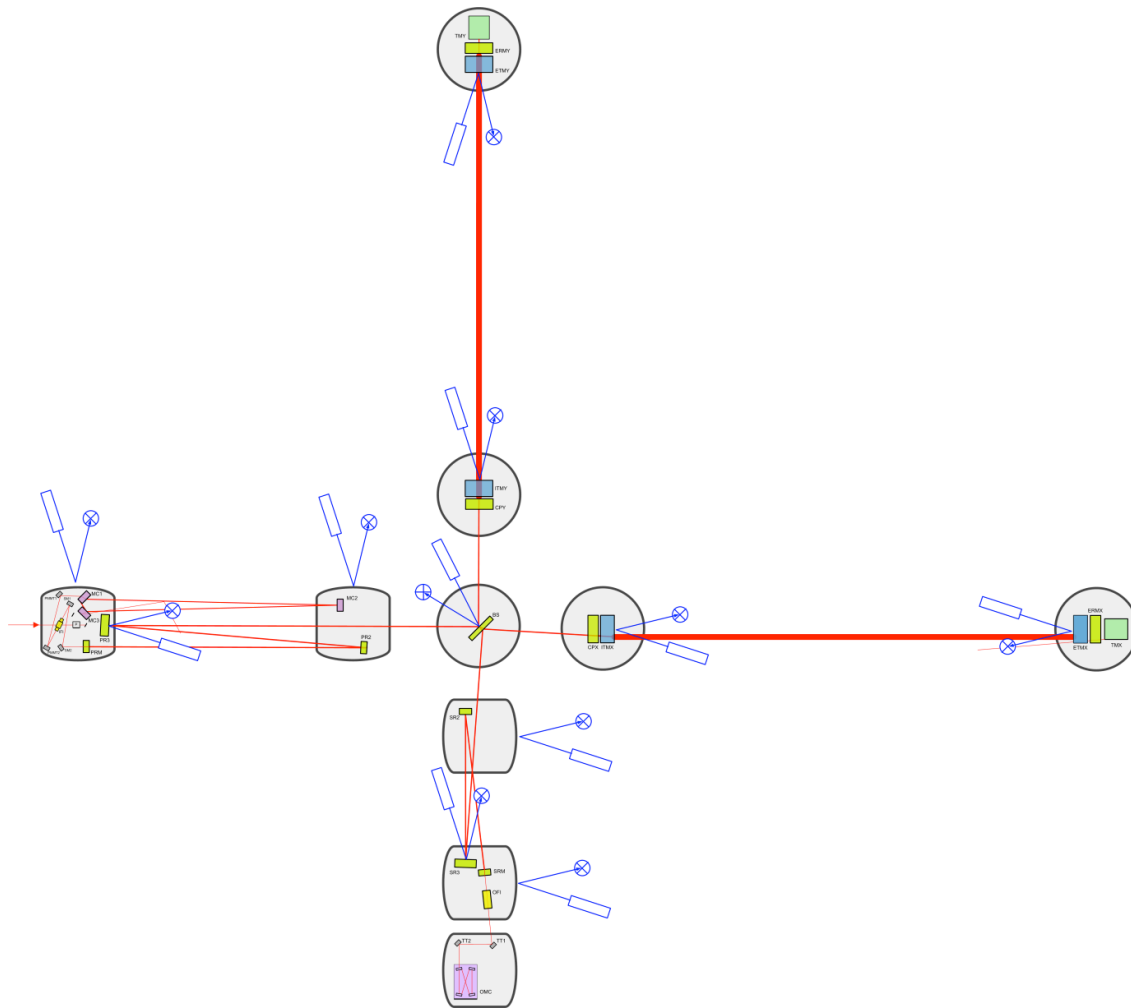


**Figure 8: Sketch of the locations of optical levers for H1 and L1. Locations for H2 are essentially the same, but includes the folding mirrors.**



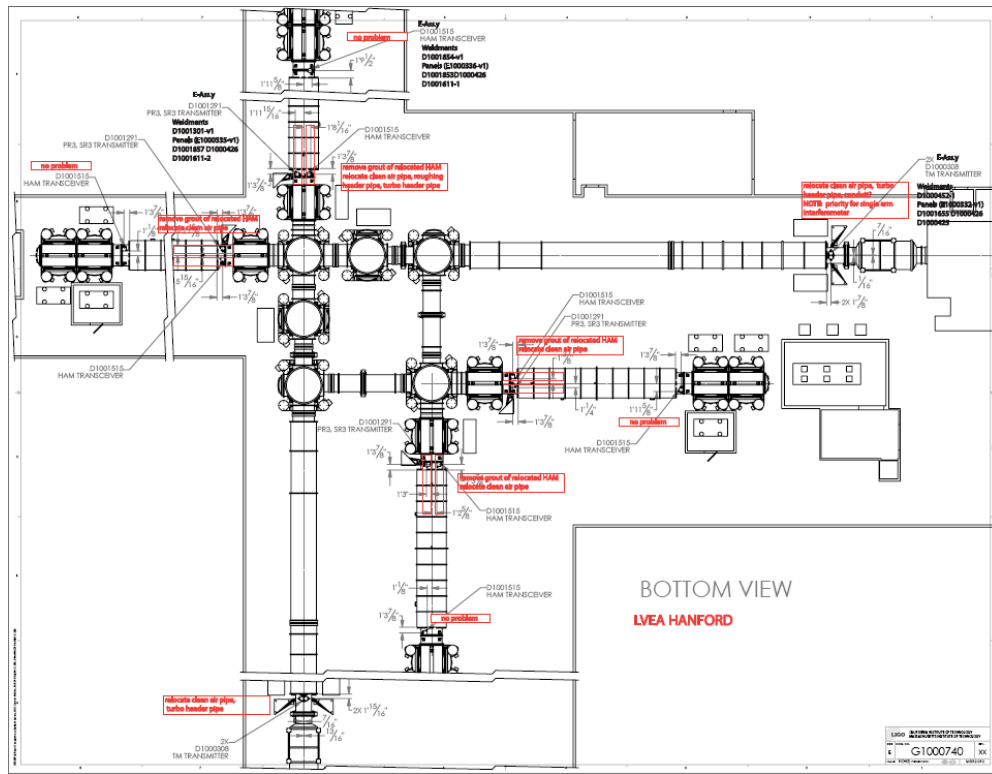


Figure 10: Bottom view of the floor occupancy, as if you were inside the concrete slab and looking up.

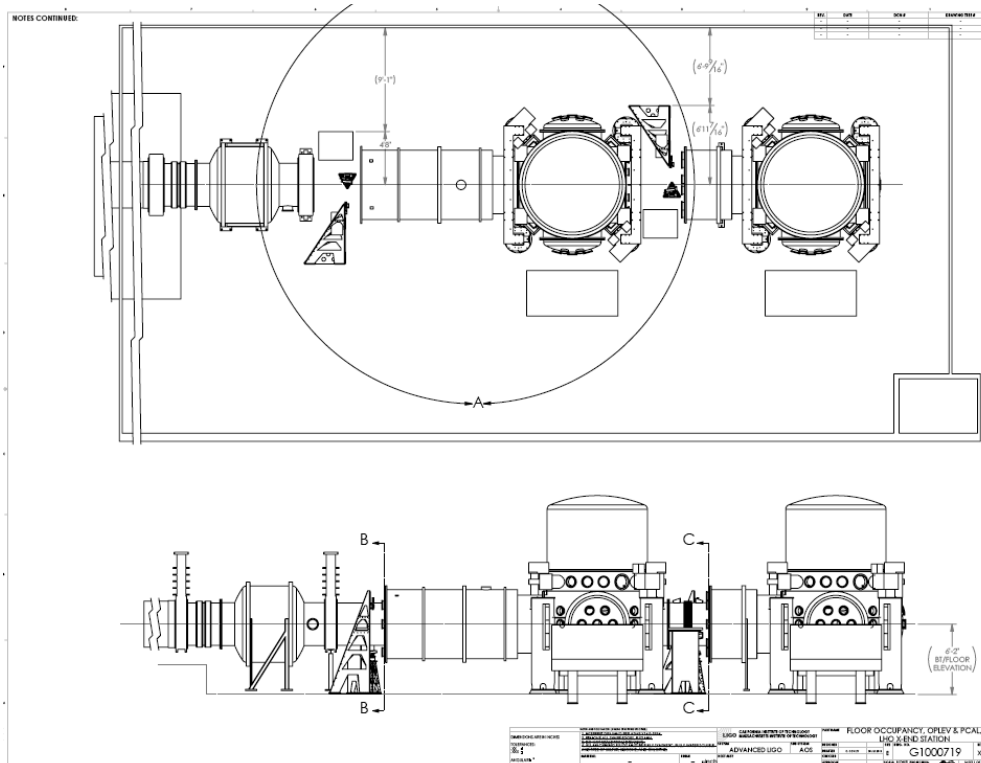
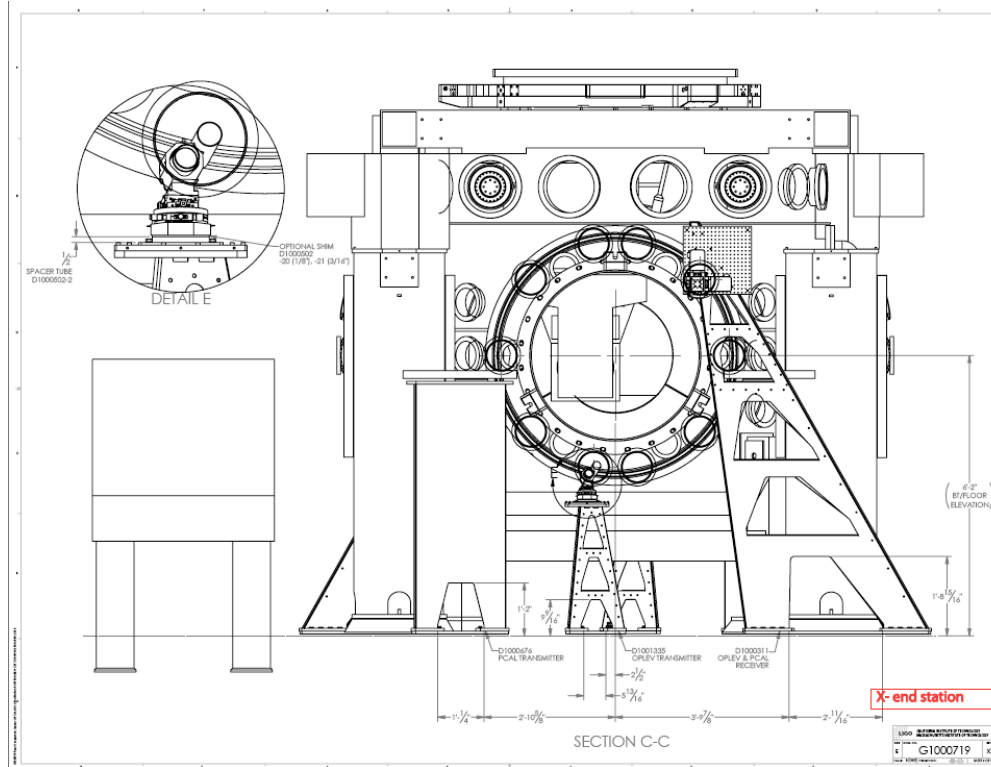
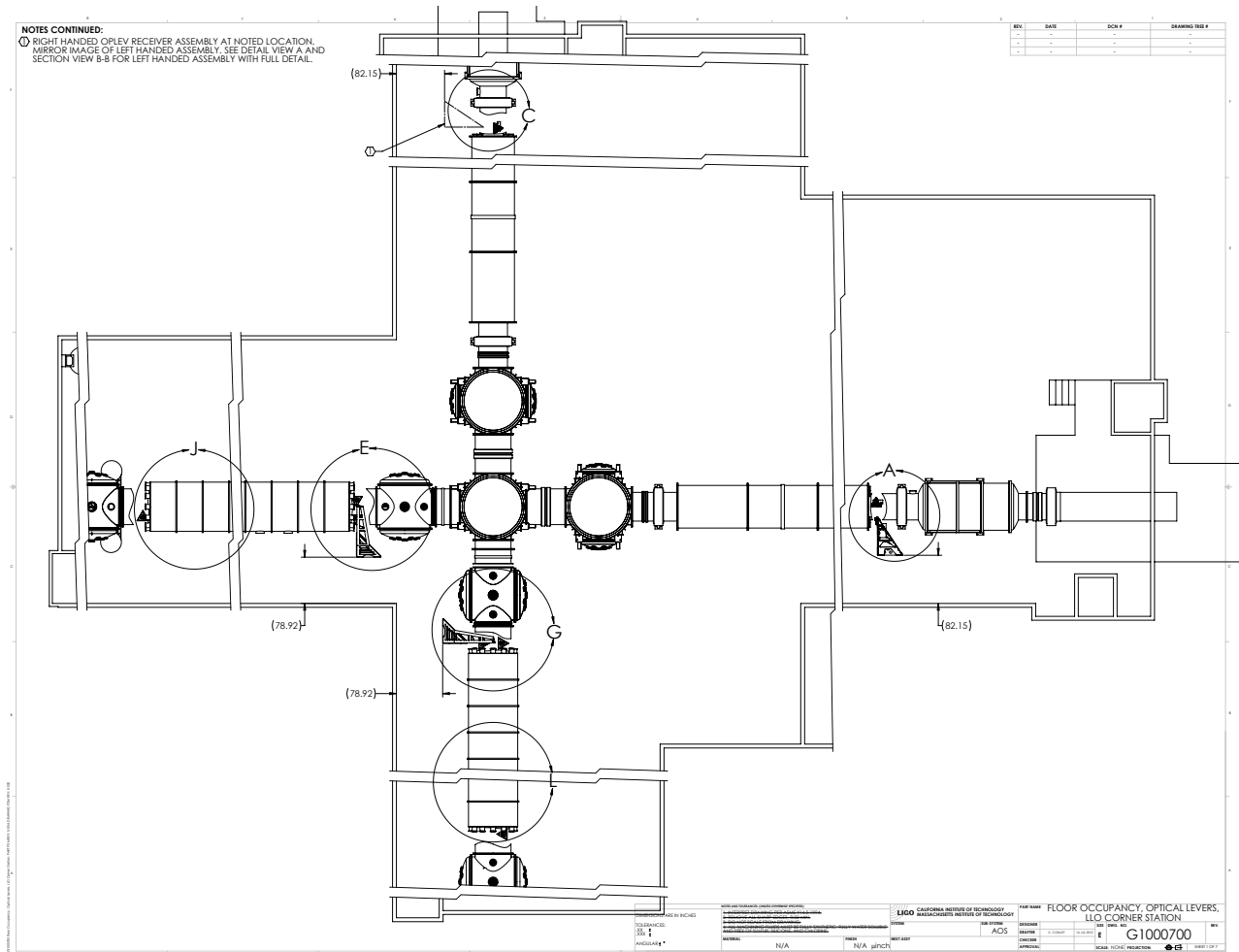


Figure 11: Typical pylon positioning around the beam pipe, LHO X-End station.





**Figure 13: Closeup of launching and receiving pylons at an X-End station, showing their positioning relative to the viewports.**



**Figure 14: Floor occupancy drawing for L1, the Livingston Corner Station.**

#### 4.4.2 LSC

Optical levers will only be used to establish mirror alignment prior to interferometer lock acquisition. No use of optical levers is foreseen (besides monitoring) for interferometer controls during normal operation.

#### 4.4.3 CDS

Cables carrying output signals will be routed to a position in the LVEA that is yet to be determined by CDS.

#### 4.4.4 Interface control document

#### 4.4.5 SLC

Having decided to maintain the present LIGO laser light source, no change in viewport or coatings is required.

### 5 Drawings

E-drawings are used as top assembly drawings showing the assembly of off-the-shelf mechanics on the fabricated parts. Weldment drawings show the assembly of the individual folded sheet metal panels forming each pylon. Drawing numbers are indicated near the illustration for each pylon.

Assembly and fabrication drawings are at [C1001526](#). The complete drawing set is listed [D1001244](#).

The models for pylons and their optics components are available in the following locations.

Test mass	transmitter	<a href="#">D1000308</a>
Test mass	receiver (LH)	<a href="#">D1000311</a>
Test mass	receiver (RH)	<a href="#">D1001212</a>
Photon cal.	transmitter	<a href="#">D1000676</a>
Recyclers	transmitter	<a href="#">D1001291</a>
Recyclers	receiver	<a href="#">D1001047</a>
HAM	transreceiver	<a href="#">D1001851</a>

Refer to document change notice [E1000182](#) for up-to-date drawing package.

### 6 Design analysis

#### 6.1 Optical

In designing the launching telescopes, we of course calculated the beam profile out to the target optic and back to the QPD. We set up a prototype telescope in the basement of Bridge Hall at Caltech, running the beam down the hall and back to a QPD. Sure enough, the return spot was exactly the size we calculated it would be.

Michael Enciso's did a SURF project on this and wrote two nice summaries. They can be found in the dcc at [T1000593](#) and [T1000559](#).

#### 6.2 Electronic

We want to keep the noise at the output of the receiver boxes relatively low. Ideally this noise should be dominated by the shot noise in the photocurrent – a fundamental noise source - and not by any technical noise source related to, say, the opamp in the active current-to-voltage converter.

The shot noise of a photocurrent  $I$  is

$$\delta I_{shot}(f) = \sqrt{2eI}$$

where  $\delta I_{shot}(f)$  is the power spectral density of the photocurrent, in Amperes per root Hertz,  $I$  is the photocurrent in Amperes, and  $e$  is the charge of an electron in Coulombs. The photocurrent is just the incident light power times the responsivity of the photodiode. The responsivity is about 0.45 at 670 nm, and the incident light power is 4 mW times the reflectivity of the sensed optic at 670 nm, a value that ranges from 6% to 40% [cite Coyne, T1000390].

For an optic with 40% reflectivity, the photocurrent is

$$\begin{aligned} I &= (0.45 \text{ A/W})(4 \times 10^{-3} \text{ W})(40\%) \\ &= 7.2 \times 10^{-4} \text{ A} \end{aligned}$$

A transimpedance of  $10k\Omega$  converts this to 7.2 V, which is well within the range an LT1125 can handle.

For an optic with only 6% reflectivity, the photocurrent is

$$\begin{aligned} I &= (0.45 \text{ A/W})(4 \times 10^{-3} \text{ W})(6\%) \\ &= 1.08 \times 10^{-4} \text{ A} \end{aligned}$$

which has a shot noise of

$$\begin{aligned} \delta I_{shot}(f) &= \sqrt{2(1.6 \times 10^{-19} \text{ C})(1.08 \times 10^{-4} \text{ A})} \\ &= 5.9 \times 10^{-12} \text{ A}/\sqrt{\text{Hz}} \end{aligned}$$

The same  $10k\Omega$  transimpedance used above turns this into a voltage noise of

$$\delta V_{shot-eq}(f) = 5.9 \times 10^{-8} \text{ V}/\sqrt{\text{Hz}}$$

Which is close enough to the 100 nV/rtHz noise floor specified in the Design Requirements Document.

Johnson noise in the transimpedance resistor is

$$\begin{aligned}
 \delta V_{\text{Johnson}}(f) &= \sqrt{4k_B T R} \\
 &= \sqrt{4(1.38 \times 10^{-23} \text{ J/K})(300\text{K})(10\text{k}\Omega)} \\
 &= 1.29 \times 10^{-8} \text{ V}/\sqrt{\text{Hz}}
 \end{aligned}$$

which is well below the shot noise.

Current and voltage noise of an LT1125 opamp are shown in Figures X and X. Voltage noise is well below shot noise down to at least 0.1 Hz, which is entirely sufficient for our purposes. Current noise is somewhat higher due to the bipolar inputs of this opamp, but it is still below the shot noise at frequencies above 10 Hz. If we want to do better at lower frequencies, we need to go to a different opamp.

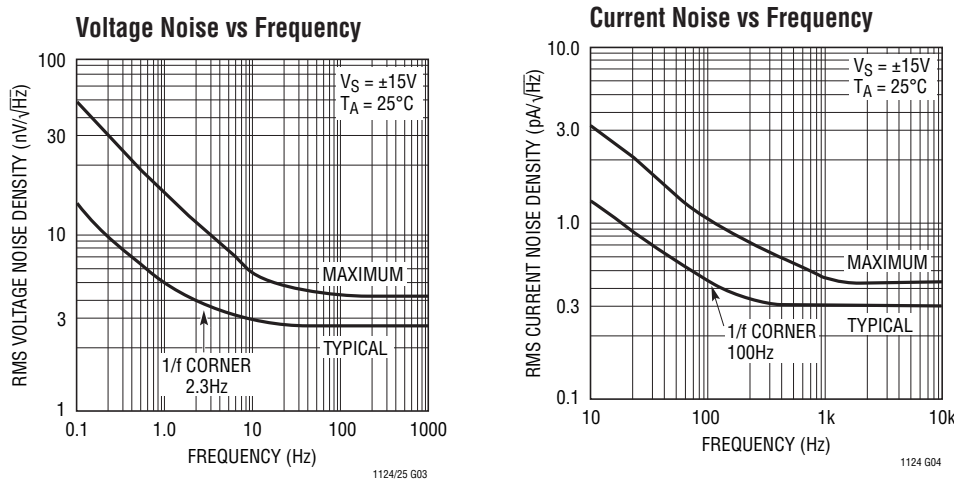


**Figure 15: Voltage- and current-noise curves for the LT1125 operational amplifier.**

### 6.3 Mechanical

We tested a mid-sized prototype pylon, found no issues with fabrication or with vibration or structural functions. To check for mechanical resonances, we placed microphonic sensors on the mid-sized prototype and tapped it with a hammer. Before we installed the constrained-layer damping material, you could hear and feel resonances when the pylon was struck. Now that the damping material is in place, you get a dull “thud” anywhere we tried pinging it. Tim McDonald quantified this lack of mechanical response and posted his results in the dcc at [T1000531](#). The first resonant frequency of this mid-sized (6 ft.) pylon was 37 Hz with very low Q-factor in a dogged-down configuration (not grouted) and with full pointing mechanism and optical payload. This high frequency is to be compared with the few Hz of some of the present LIGO tall optical lever structures.

Because all launchers are about half its height, we expect resonant frequencies even higher than this.

The taller pylons (test mass receiver and recycler receiver, 8 and 10 feet tall) will have lower resonant frequency. This frequency reduction is mitigated by the fact that the payload is smaller and the structure is made with thicker gauge. All resonances will be efficiently damped like in the prototype by the same constrained-layer rubber and aluminum foil damping sheets. In any event, mechanical resonances in these tall pylons are of much less concern than in the shorter ones. The sensitivity to vibration on the receiver side is much smaller than that on the launcher side because there is no optical lever amplification.

## 7 Tooling Support for Installation

### 7.1 Fixturing and alignment jigs and masks

A mask (acetate or mylar) over the viewport, marking the desired position of the injected beam, will be used to position the launching telescope pylon. Once the telescope faces its mark on the mask within a cm, sufficient positioning is achieved. This is achieved by laterally positioning the pylon on the ground horizontally, and by acting on the three vertically supporting screws of the base plate vertically. Once found, the desired position is marked, the pylon removed, rock bolts are sunk in the concrete, the pylon repositioned and bolted. (See assembly procedure [LIGO-E1000352-v1](#).)

A similar mask will be used at the other end to position the receiver pylon.

The grout on the pylon footings will be case only after certification of the optical lever good functioning.

### 7.2 Aligning beams

The launching beam will be aimed to the target mirror ~~either with the help of pointing telescopes (test mass case) or~~ manually. The viewfinder telescopes shown in the original design were deleted by decision of the optical lever subsystem lead and the chief engineer. It was decided that these telescopes were no longer necessary or useful (see RODA M1100275).

A similar mask will be used on the viewport of the receiving end. Once the reflected beam hits the mask with 1 cm precision, sufficient alignment is achieved.

### 7.3 Calibration of sensors

Calibration of radians/volt is obtained by scanning the QPD over the static beam (during interferometer lock) with the stepper motors (or the picomotors taking into account the lever arm between the tip/tilt mirror and the quadrant photodiode).

## 8 Repair scenarios

### 8.1 Laser replacement

A failing laser, signaled by instability or loss of signal on the QPD, can be easily swapped by disconnecting a standard APC fiber connector.

### 8.2 Fiber replacement

The fiber leading to the launching telescope should never be replaced because it leads to loss of the mirror alignment memory. In case of physical damage the fiber can be swapped with a new one of equal length. If properly done by a trained person, the beam should still reach the QPD, but fine mirror alignment would be lost.

### 8.3 Stepper- and pico-motor replacement

Ditto, a replacement of stepper or pico motors leads to loss of the mirror alignment information.

### 8.4 Recalibration

Realignment of the QPD on the beam will be necessary in case of fiber or motor replacement, but recalibration is not necessary.

## 9 Requirements on Susystem Components

- Pylon rigidity sufficient not to amplify the seismic motion is required. It is achieved with light pyramidal pylons.
- Rigidity of the launching telescope better than 1 microradian is required. It is achieved by custom locking mechanism on the micrometric tip/tilt stage.
- Lifetime light source exceeding the infrastructure lifetime is desirable. It is not achieved with the chosen lasers. Scheduled replacements will be necessary every one or few years.

## 10 Safety Approach – Designs, Plans, Procedures

The optical levers do not entail any particular danger. The collimated light involved about the level of that of a laser pointer (less than 5 mW) and they are not considered dangerous. Some of the optical lever structures are tall (up to 3 meters), but the dangers of fall can be easily mitigated by means of proper climbing instruments (ladders). The risks are analyzed in the risk analysis document.

### 10.1 Mechanical

The only mechanical risk is during handling of the pylons, which is easily avoided if the operations are performed by trained crane operators with proper hoisting equipment (lifting belts).

## 10.2 Optical

On top of being weak, the light beams are collimated to high density only in proximity of the quadrant photodiodes, where they are contained by protection boxes.

## 10.3 Electrical

The optical levers use no voltage higher than 15 V, and with small amperage. There is no safety issue.

## 10.4 Viewports

Every viewport is protected with the standard LIGO guillotine shutter, to be opened only after a protection box encloses the opening. The protection box, solidly mounted to the pylon structure, but not touching the guillotine shutter, is designed to contain debris in case of shattering viewport.

# 11 Test Plans and Test Schedule

## 11.1 Calibration plan

Once the beam reflected on the target mirror reaches the quadrant photodiode, the angular sensitivity of the optical levers is easily obtained by scanning the beam spot with the stepper motor (or picomotor) stage and dividing the physical relative displacement of the spot with respect to the photodiode by the optical lever length. The physical quadrant photodiode signal would be read out by the aLIGO data acquisition system.

## 11.2 Noise measurement plan

The noise measurements of [Mohana report TBF] will be repeated using the aLIGO data acquisition system as soon as installed or by a local spectrum analyzer.

## 11.3 Prototype pylon mode frequency measurements

These have been done on a mid-sized pylon, and the results are reported elsewhere in this document.

## 11.4 Fit checks

Fit check of the pylons will be performed at the time of installation. The larger pylons that fit around the beam pipe will be mounted as close to the beam pipe as possible (with at least 2 cm clearance) to reduce occupancy in the corridors. The breadboard supporting the stepper motors and quadrant photodiodes allows for lots of positioning leeway. We rely on design parameters and model fitting to fit the launcher pylons below the beam pipes. A 5 cm reserve spacer between the pylon and the telescope mechanism can be used to reduce the pylon effective height in case of mistake.

## 11.5 Spec compliance checks

Check that light spots are correctly reaching the quadrant photodiodes.

Check electronics noise level and verify that it is below 100 nV/ $\sqrt{\text{Hz}}$  at frequencies of interest.

After the interferometer is commissioned and can be locked for several hours at a time, stability of the combined system of the suspended optic and its associated lever should be checked against the wavefront angular sensing to verify that it meets the 1 micro-radian per hour spec. This test operates on the assumption that the suspended optic is stable and that the majority of the observed drift would be due to the optical levers.

A plan needs to be developed to check the position-to-angle coupling spec. Such a test would require an independent measure of the angular motion of the optic (e.g. WFS) and seems impractical before the interferometer is commissioned and locking for a decent length of time.

## 12 Deliverables

See Appendix A for a list of deliverables by manufacturer and site.

## 13 Software

The hardware delivers the signals from the individual photodiode quadrants. Calculation of pitch and yaw signals, normalization, and laser-power monitoring must all be done in software. Rolf Bork has developed an object-oriented programming environment for writing interferometer control software using simulink. Once the appropriate DAQ channels are accessed, the code for reading out the optical-lever signals will look something like this.

```
global_variables{
    lever_arm($ARG),
    linear_response($ARG),
    power_response($ARG),
    current_monitor($ARG)};

selected_optic = user_input(pulldown_menu);
L = lever_arm(selected_optic);
R = linear_response(selected_optic);
k = power_response(selected_optic);
j = current_monitor_conversion(selected_optic);

q1 = read(voltage1);
q2 = read(voltage2);
q3 = read(voltage3);
```

```

q4 = read(voltage4);
current = read(voltage5);

sum = q1 + q2 + q3 + q4;
If(sum<threshold)
    {set_alarm(sum);
    break;}
else
    {pitch = (q1 + q2 - q3 - q4)/(sum * R * L);
    yaw = (q1 - q2 - q3 + q4)/(sum * R * L);
    send_to_medm_display(pitch, yaw, k * sum, j * current);
    send_to_medm_crosshairs(pitch, yaw);}

```

**Figure 16: Pseudocode for optical-lever readout.**

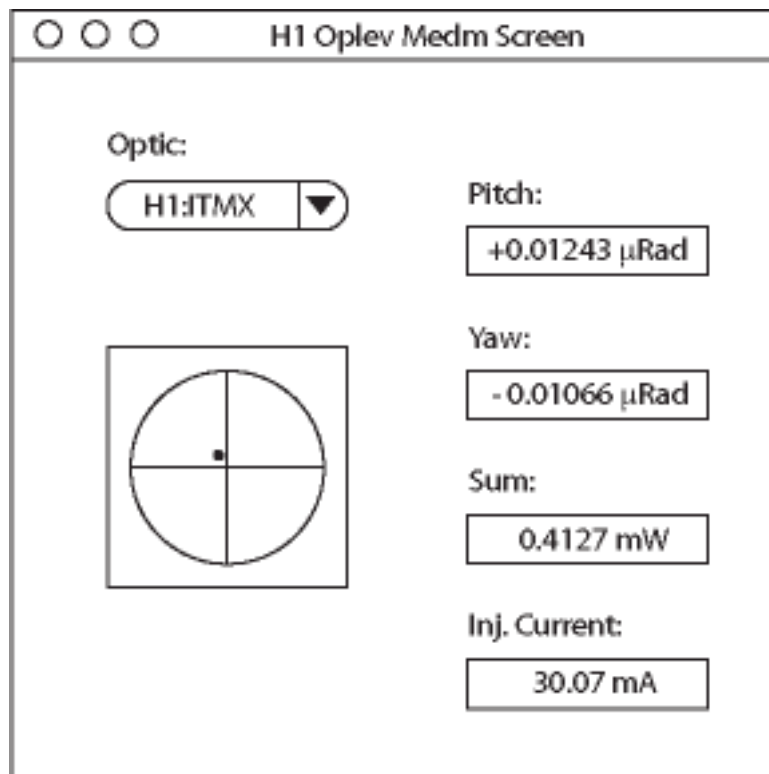


**Figure 17: Example interface screen for a single optic, chosen from user-selected pulldown menu.**

Software associated with the local position controllers of either the QPDs or the launching telescopes is provided by the vendor and does not interface with any other elements.

## 14 Cost estimates

The largest expense (estimated to ~750k\$) is represented by the pylons, which are designed to our drawings, and which will be procured with a standard RFQ process.

The second most expensive items are the telescope and quadrant photodiode aiming mechanisms (evaluated at ~200k\$), which are catalog items that will be acquired with a non competitive procurement.

The third most expensive items are the laser sources (estimated at 135k\$). Fifteen new lasers need to be procured from the previous manufacturer (estimated at 15\*8k\$) and the existing ones to be refurbished with new laser heads and APC fibers (estimated at 30\*0.5k\$). A 25% of spares is deemed necessary due to the limited laser lifetime. Bids have been requested.

The fourth most expensive items are the telescopes themselves (evaluated at ~50k\$), which are catalog items that will be acquired with a noncompetitive procurement.

All other items are off-the-shelf components with marginal costs.

### 14.1 Summary of costs

Pylons	~750k\$
Micrometric mechanisms	~200k\$
Lasers	~135k\$
Telscopes	~50k\$
Miscellaneous	balance

### 14.2 Compatibility with cost book

Barring surprises with the pylon and laser bids, the costs should remain within cost book.

### 14.3 Changes since the PDR

The basic cost analysis remains essentially unchanged from the one given in the preliminary design document.

The change request M1000226 concerns the change of budget to account for the present cost evaluation. The cost adjustment reflects our best present cost estimates.

## 15 Fabrication and Purchasing of Parts

### 15.1 Parts List

[C1001654](#) contains all the parts except the individual pylon components, which are detailed in the drawing package.

## 15.2 Acquisition of parts and components

We have identified the necessary catalog components, contacted the relevant providers, and obtained informational quotations and delivery times. Details are specified in the parts list. Final quotations will be requested after final design approval.

One set of components still remains to be designed and fabricated, and those are the optics and viewport protection boxes to be mounted on top of the pylons. They are simple bent sheet metal boxes, which will be designed together with the vertical views of the floor occupancy drawings, produced and then adapted at necessity. This part of the design will complete the optical-lever interface to the rest of the observatory (see Section 8.1).

The statements of work for the pylons can be found in the DCC page [C1001526](#) and the DCN page [E1000182](#).

## 15.3 Production

Companies who could potentially produce the mechanical components are listed in the document [C1001537](#), “Optical levers fabricator list.” We visited them to make sure they are all capable of doing the job and are interested in bidding.

There are no critical materials involved in the fabrication.

## 16 Installation

### 16.1 Locations (Final Interface Control)

The most bulky components are the pylons, which will be delivered in crates. They should be inspected at delivery, or before shipment, for dimensional tolerance, and stored in the crates until installation. Storage of the crated pylons will require an estimated 26 square meters of indoor space per interferometer. The off-the-shelf micrometric mechanisms and optical components should be stored in clean cabinets until installation.

The interface control documents include the floor occupancy plans, which give the relative positioning of all optical levers. Examples were given earlier in this document, and the complete floor occupancy drawing numbers are,

For Livingston

[G1000700](#) corner station

[G1000701](#) X-end

[G1000702](#) Y-end

For Hanford

[G1000740](#) corner station

[G1000719](#) X-end

[G1000739](#) Y-end

Besides the actual floor occupancy, they also include vertical views defining the interface of the optical components, their protection boxes and their respective viewports. The vertical views are necessary at the time of actual installation.

## 16.2 Installation plans and procedures

The complete installation plans and procedures can be found at [E1000352](#).

## 16.3 Grouting

The two dirty operations to be performed in the LVEA are the jackhammering of the old grout of the three repositioned HAM, to make space for the optical lever pylons, and the drilling of the anchoring holes for the pylons. Both will best be done with temporary tenting and underpressure (vacuuming). As accidental dust emission cannot be excluded, all operations should be done with sealed vacuum chambers. The grout removal task is left to the care of the local de-installation staff. Drilling of the anchoring holes needs the presence of the optical lever team and can be done with vacuumed cups around the drilling bits to minimize LVEA exposure.

Grout should be mixed outside the LVEA and brought in only in its wet status, to avoid dusting the LVEA.

## 17 Final-Design-Review Checklist

Final requirements - any changes or refinements from PDR?

Section 1.1 of this Final Design Document (FDD)

Resolutions of action items from PDR

Section 3 of FDD

Subsystem block and functional diagrams

Figure 5 of FDD

Drawing package (assembly drawings and majority of remaining drawings)

Section 5 of FDD

Final parts lists

Section 15.1 and Appendix A of FDD

Final specifications

Section 2 of FDD

Final interface control documents

Sections 4.4 and 16.1 of FDD

Signed Hazard Analysis

Posted at [E1000351](#).

Design analysis and engineering test data

Section 6 of FDD

LIGO-T1000531-v1

Software detailed design

N/A (Section 13 of FDD)

Final approach to safety and use issues

[E1000351](#) (hazard analysis) and 16.2 (installation plans) of FDD

Production plans

Section 15.3 of FDD

Plans for acquisition of parts, components, materials needed for fabrication  
 Section 15.2 of FDD

Installations plans and procedures  
 Section 16.2 of FDD

Preliminary hardware test plans  
 Section 11 of FDD

Preliminary software test plans  
 N/A

Cost  
 Section 14 of FDD  
 Change request LIGO-M1000226

Fabrication, installation and test schedule  
 Section 19 of FDD

Lessons learned, documented, circulated  
 Section 19 of FDD

Problems and concerns  
 Section 6.3 of FDD ("None relevant")

## 18 Schedule

LLO Installation Schedule [G1000013](#) (updated 8/20/10)

LHO Installation Schedule [G1000061](#) (updated 8/20/10)

## 19 Lessons Learned and Documented

Analyzing the old optical levers we found that their limitations came from mechanical weakness of the pylon footings (amplifying the seismic motion), beam routing defects, air turbulence, and above all laser mode instabilities.

The pylons have been completely redesigned, with a much more rigid pyramidal structure and grouted footing. This completely solved the problem.

Instead of routing the expanded launched beams with folding mirrors, we directly aimed the launching telescopes with very rigid tip/tilt mechanisms. This eliminated vignetting of the beam, reduced Airy rings, and resulted in a much more rigid system.

Positioning the aimed launching telescopes as close as possible to the viewports minimized the air turbulence problem.

By far the largest problem comes from the modal instabilities of the laser feeding into the fiber. These instabilities, generated by acoustic or mechanical excitation of the fibers but also by simply scanning the laser power, were shown to generate launched beam angular noise much in excess of the requirements (i.e. several microradians). The physical effect derives from interference of different modes generating stripes on the light spot at the end of the optical levers. The fibers are nominally monomode fibers, but obviously transmit more than one mode over the short distances involved in the experimental halls. These stripes projected on the quadrant photodiode produce large angle readout variation.

It was shown that a large fraction of the modal jumping of the laser was driven by reflections on the perpendicular cut fibers, and the microphonic sensitivity of the fiber was mitigated by switching to angle cut fibers throughout (to eliminate the microphonic problem we had to get a modified laser with angle cut fiber all the way to the laser diode). Laser modal jumping could still be generated by scanning the laser power and can be expected from natural instabilities of the lasers.

The only way to positively eliminate this problem would be to use incoherent light. The proposed solution of replacing the lasers with SLEDs was rejected on the basis that the existing lasers are probably stable enough.

## 20 Risks, Problems, and Concerns

### 20.1 Late delivery

There is an actual risk that delivery be delayed, either by the review, the procuring, or the manufacturing process. The delivery times have been chosen according to the maser installation schedule, with some leeway. After that the optical levers may be late.

### 20.2 What if the pylons don't fit?

The pylon designs have been checked against the existing layout. The large pylons can be moved laterally or mounted on thicker grout if necessary. If the smaller launcher pylons are not built to spec and do not fit, they will need to be replaced.

### 20.3 Other concerns

The main concern is that there is no telling on how close a laser can be to mode instability, or when it could drift into one due to its slow power decline. A laser close to instability may become microphonic even with angle-cut fibers. A simple power fluctuation can trigger angular instabilities well outside specs and cause mirror misalignment.

## 21 Related Documents

The list of related documents is available in [E1000348](#).

## 22 Appendix A: Deliverables by site

Total quantities required from Thorlabs, destinations and delivery dates:

Item Num	pylon	Description	Total Quant	Spares	DELIVERY QUANTITIES & SCHEDULE

			ity Order ed		LIGO Hanford, WA		LIGO Living ston, LA
					1/3/11	3/30/11	2/28/1 1
1	Test mass telescope	BE20M- B  Beam Expande r	14	2	3	6	5
2	Test mass 2" ext.	SM2L20  Lens Tube	14	2	3	6	5
3	Test mass collimator adapter	AD12F  SM1 Adapter for Collimato rs	14	2	3	6	5
4	Fiber collimator	F240AP C-A	40	5	3	26	14
5	Rec./HAM telescope	BE03M- B  Beam Expande r	20	2	0	13	7
6	Rec./HAM/ BS collimator adapter	Special part	30	7	0	20	10
7	BS/FM	BE02M-	5	2	0	5	2

	telescope	B						
		Beam Expander						
Item Num	Parts needed per each beam	Description	Total Quantity To Order	Spares	LIGO Hanford, WA		LIGO Livingston, LA	
					1/3/11	3/30/11	2/28/11	
1	AC508-300-B	Lens Ø50.8 mm, f=300.0 mm	<b>8</b>	<b>2</b>	3	2	3	
2	AC508-200-B x2	Lens Ø50.8 mm, f=200.0 mm	<b>16</b>	<b>4</b>	6	4	6	
3	ACN127-025-B	Lens Ø12.7 mm, f=-25.0 mm	<b>8</b>	<b>2</b>	3	2	3	
4	SM1A2 x2	adapter External SM1 Internal SM2	<b>16</b>	<b>4</b>	6	4	6	
5	SM1A9 x2	Adapter External C-Mount Internal SM1	<b>16</b>	<b>4</b>	6	4	6	
6	SM2L03 x2	SM2 Tube, 0.3" Thread Depth	<b>16</b>	<b>4</b>	6	4	6	
7	SM2L05 x3	SM2 Tube, 0.5" Thread Depth	<b>24</b>	<b>6</b>	9	6	9	

8	SM2L10 x5	SM2 Tube, 1.0" Thread Depth	<b>40</b>	<b>10</b>	15	10	15
9	SM2L20 x2	SM2 Tube, 2.0" Thread Depth	<b>16</b>	<b>4</b>	6	4	6
10	SM2L30	SM2 Tube, 3.0" Thread Depth	<b>8</b>	<b>2</b>	3	2	3
11	SM2L50 custom made	SM2 Tube, 5.0" Thread Depth	<b>8</b>	<b>2</b>	3	2	3
12	SM2T1	SM2 Coupler Internal	<b>8</b>	<b>2</b>	3	2	3
13	SM2T2	SM2 Coupler External	<b>8</b>	<b>2</b>	3	2	3
14	SM2V10 x2	SM2 Adjustable Focus	<b>16</b>	<b>4</b>	6	4	6
15	AD1	Adapts Ø1/2" to Ø1"	<b>8</b>	<b>2</b>	3	2	3
16	AD2	Adapts Ø1" to Ø2"	<b>8</b>	<b>2</b>	3	2	3
17	SM2CP2 x2	SM2 End Cap	<b>16</b>	<b>4</b>	6	4	6
18	SM1A10 x2	adapter External SM1 Internal C- Mount	<b>16</b>	<b>4</b>	6	4	6
19	SM1CP2 x2	End Cap SM1	<b>16</b>	<b>4</b>	6	4	6



Total quantities required from OptoSigma, destinations and delivery dates:

Item Num	pylon	Description	Total Quantity Ordered	Spares	DELIVERY QUANTITIES & SCHEDULE		
					LIGO Hanford, WA		LIGO Livingston, LA
					1/3/11	3/30/11	2/28/11
1	Test mass launcher	Micrometric tip tilt stage (70 mm)	12	2	2	6	4
2	Test mass receiver LH	X-Y micrometric stepper motor stage 33 series LH	6	1	1	3	2
3	Test mass receiver RH	X-Y micrometric stepper motor stage 33 series RH	6	1	1	3	2
4	Recycler launcher	Micrometric tip tilt stage (40 mm)	6	2		4	2
5	Recycler receiver LH	X-Y micrometric stepper motor stage 33 series LH	4			2	2
6	Recycler receiver RH	X-Y micrometric stepper motor stage 33 series RH	2			1	1
7	HAM trans-receiver	Micrometric tip tilt stage (40 mm)	12			8	4
8	Beam splitter Folding mirror	Micrometric tip tilt stage (40 mm)	5			4	1
9		Stepper motor controllers	4		1	1	2